

Polar-Electrode-Bridged Electroluminescent Displays: 2D Sensors Remotely Communicating Optically

Xiuru Xu, Dan Hu, Lijia Yan, Shaoli Fang, Clifton Shen, Yueh-Lin Loo, Yuan Lin, Carter S. Haines, Na Li, Anvar A. Zakhidov, Hong Meng,* Ray H. Baughman,* and Wei Huang*

A novel geometry for electroluminescent devices, which does not require transparent electrodes for electrical input, is demonstrated, theoretically analyzed, and experimentally characterized. Instead of emitting light through a conventional electrode, light emission occurs through a polar liquid or solid and input electrical electrodes are coplanar, rather than stacked in a sandwich configuration. This new device concept is scalable and easily deployed for a range of modular alternating-current-powered electroluminescent light sources and light-emitting sensing devices. The polar-electrode-bridged electroluminescent displays can be used as remotely readable, spatially responsive sensors that emit light in response to the accumulation and distribution of materials on the device surface. Using this device structure, various types of alternating current devices are demonstrated. These include an umbrella that automatically lights up when it rains, a display that emits light from regions touched by human fingers (or painted upon using a mixture of oil and water), and a sensor that lights up differently in different areas to indicate the presence of water and its freezing. This study extends the dual-stack, coplanar-electrode device geometry to provide displays that emit light from a figure drawn on an electroluminescent panel using a graphite pencil.

improvements in light-emitting elements, like textiles that function as information displays or provide fashionable effects in clothing, sensors that communicate responses optically, and possibly even implantable medical devices that emit light in response to sensor input to release drugs, destroy photochemically sensitized tissue, or communicate to neurons.

Alternating current (AC) electroluminescent light sources likely provide the simplest flexible and uniformly light-emitting panels. They can be prepared using inexpensive screen-printing and have, for decades, occupied a niche segment of the flat-panel display and lighting markets, as one of the earliest products for soft electronics.^[12–14] With recent advances in printing technologies, such as 3D printing, a new device architecture that allows easy printing onto any substrate would provide further simplification and modularity for soft electronic devices.

The field of soft electronics is rapidly progressing as a result of recent advances in functionally generalized, modular device architectures for various applications, including wearable electronics,^[1,2] implantable devices,^[3,4] sensory skins,^[5,6] soft robotics,^[7,8] and energy generation and storage systems.^[9–11] Various applications in soft electronics could benefit from

We will describe and demonstrate a novel device concept that can be deployed for a range of modular AC-powered electroluminescent (EL) and light-emitting sensing devices. This concept is simple, easily deployed, and scalable; can utilize various light emitters and other device components; and can provide a host of sensing functions that result in light emission. The new devices comprise four components:

Dr. X. Xu, D. Hu, Prof. C. Shen, Prof. Y. Lin, Prof. H. Meng
School of Advanced Materials
Peking University Shenzhen Graduate School
Shenzhen 518055, China
E-mail: menghong@pkusz.edu.cn

Dr. L. Yan, Prof. W. Huang
Key Laboratory of Flexible Electronics and Institute
of Advanced Materials
Jiangsu National Synergetic Innovation Center for Advanced Materials
Nanjing Tech University
Nanjing 211816, China
E-mail: iamwhuang@njtech.edu.cn

Prof. W. Huang
Shaanxi Institute of Flexible Electronics
Northwestern Polytechnical University
Xi'an 710072, China

Prof. S. Fang, Prof. C. S. Haines, Dr. N. Li, Prof. A. A. Zakhidov,
Prof. R. H. Baughman
Alan G. MacDiarmid NanoTech Institute
University of Texas at Dallas
Richardson, TX 75083, USA
E-mail: ray.baughman@utdallas.edu

Prof. Y.-L. Loo
Department of Chemical and Biological Engineering and the Andlinger
Center for Energy and the Environment
Princeton University
Princeton, NJ 08544, USA

 The ORCID identification number(s) for the author(s) of this article can be found under <https://doi.org/10.1002/adma.201703552>.

DOI: 10.1002/adma.201703552

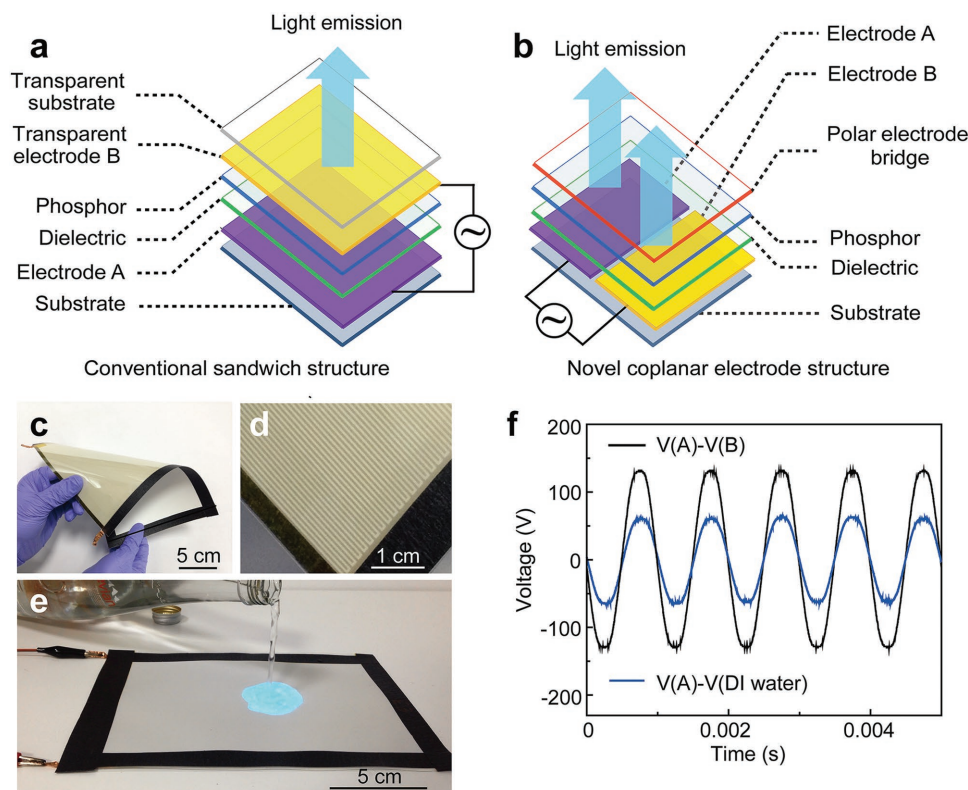


Figure 1. Schematic illustrations and photographs comparing a conventional sandwich electroluminescent light source (S-ELS) with a polar-electrode-bridged electroluminescent light source (PEB-ELS). Illustrations comparing a) an ordinary S-ELS with b) a PEB-ELS. c) Photograph showing the flexibility of a large-area panel for a PEB-ELS. d) Higher magnification photograph showing the electrodes on the backside of the PEB-ELS (which have widths of 0.45 mm and gaps of 0.40 mm). e) Pouring drinking water onto the upper PEB-ELS surface causes the contacted surface to emit light. f) Oscilloscope recording of the AC voltages of a PEB-ELs, measured between electrodes A and B (black) and between electrode A (or electrode B) and the polar electrode bridging layer of deionized water (blue).

a pair of electrodes that are optionally parallel and coplanar, light-emitting layers, dielectric layers, and a modulating electrode layer made of a selected polar material or an electronically conducting film. Opposite electrodes for power input are in different device layer stacks, rather than in the same device stack, as in conventional light-emitting devices.

When this modulating electrode is a dipolar liquid or dipolar solid, the electroluminescent device is called a polar-electrode-bridged electroluminescent light source (PEB-ELS). Using this device structure and a polar material as an electrode bridge, various types of alternating current devices are demonstrated. These include an umbrella that automatically lights up when it rains, a display that emits light from regions touched by human fingers (or painted upon using a mixture of oil and water), and a sensor that lights up differently in different areas to indicate the presence of water and its freezing.

A conventional AC electroluminescent light source (Figure 1a) comprises a phosphor layer in a polymer binder along with one or more layers of dielectric insulator, sandwiched between a metal back electrode and a transparent conducting front electrode (e.g., indium tin oxide) (Figure 1a).^[15,16] We call this conventional device a sandwich electroluminescent light source (S-ELS). In contrast, the electrodes used for energy injection in our PEB-ELS (Figure 1b) can be coplanar and nonoverlapping, and on the back of the device, so neither

of these electrodes is required to be optically transparent. While the S-ELS comprises a single layer stack, the PEB-ELS can be functionally viewed as comprising two stacks of layers, wherein these stacks electrically operate in series to provide light emission from both stacks. Although the Figure 1b illustration shows layer continuity between the two stacks for phosphor and dielectric layers, and this continuity is useful for convenient device fabricability, it is not required for device function. However, the modulating electrode (which is a polar liquid, like water, or a polar solid) is called a bridging electrode, since it must bridge between the two electrode stacks in order to enable light emission. The transparency of this polar bridging electrode is critically important for device operation, but is easily realizable since there are so many useable optically transparent polar liquids and solids.

Using the device architecture of Figure 1b, we fabricated a fairly large panel ($\approx 15.0 \times 21.0 \text{ cm}^2$) of ≈ 250 PEB-ELs by screen-printing an array of parallel coplanar silver electrodes on a flexible polyethylene terephthalate (PET) substrate, followed by sequential printing of a dielectric layer and a phosphor layer (Figure 1c,d). The silver electrodes had 0.45 mm widths and 0.40 mm gaps between electrodes. Without the presence of a polar electrode bridging layer, no light emission occurred when 132.2 V at 1 kHz was applied. However, the contacted panel region emitted light when water from a bottle of drinking

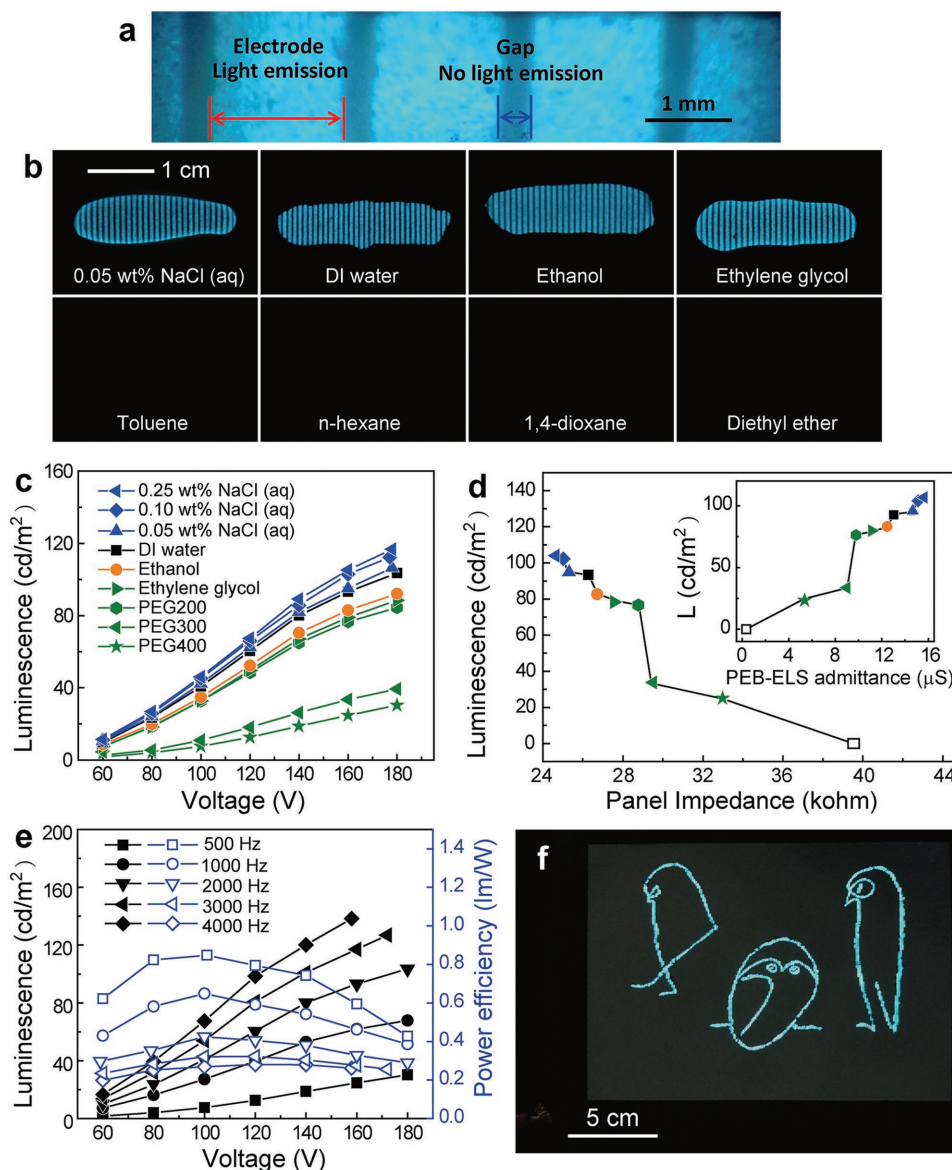


Figure 2. Effects of bridging materials, voltage, and frequency on the performance of PEB-ELSs. a) Photograph of a working PEB-ELS with 1.5-mm-wide electrodes and 0.4-mm-wide interelectrode gaps. b) Photographs of PEB-ELSs operating in the dark using various modulating liquids. c) Luminescence versus applied voltage for various polar electrode bridge liquids on PEB-ELSs that are operated at 2 kHz. d) The dependence of PEB-ELS luminescence (for 160 V, 2 kHz voltage) on panel impedance for the polar electrode bridges of (c), using the same symbols for different compositions as in (c). The data point for zero luminescence (an open square) is for diethyl ether. Inset: The dependence of luminescence (L) on the admittance of the liquid-contacted area. e) The dependence of luminescence and power efficiency (for different applied frequencies) on applied voltage for a PEB-ELS that uses DI water as the polar electrode bridge. f) Photograph of light emission (100 V at 2 kHz) from a Picasso-inspired image that was drawn on the panel of Figure 1c,d using a graphite pencil. All results except those in the inset of (d) are for the fully powered 15 × 21 cm entire panel area, with luminescence and admittance determined for the 2 × 4 cm panel area covered by bridging liquid, and the impedance being that of the entire panel.

water (Evian Natural Spring Water) was poured on top of the PEB-ELS panel (Figure 1e). Contacting the top of the panel with deionized (DI) produced essentially the same light emission. The measured voltage between electrode A and electrode B was 132.2 V, while that between modulating DI water and electrode A or B was 60.4 V (Figure 1f), indicating that the potential drop along the length of the DI water bridge was 11.4 V.

Figure 2a is a high-resolution photograph of light emission from a PEB-ELS panel in which the electrodes are 1.5 mm wide

and have a 0.4 mm electrode gap, when using DI water as the liquid of the bridging electrode. This image shows that light emission occurs in the overlapping area between liquid and underlying metal electrodes, rather than in the gaps between metal electrodes. This differentiates the behavior of our devices from that reported for other coplanar electrode devices, such as electrochemical cells,^[17] photovoltaics,^[18] and light-emitting field-effect transistors,^[19] where light is emitted in the gap between metal electrodes.

To further investigate the relationship between light emission and position of the polar material on the device, we constructed a two-electrode PEB-ELS having wider electrodes (3.0 mm) and a 0.4 mm interelectrode gap. We carefully applied single DI water droplets on top of the electroluminescent layer that was above the current injecting electrode. No light emission occurred as long as the droplets were confined to be above a single electrode (and not connected over the gap “g”). Only after the water droplets spread to bridge the gap between the two adjacent A(+/-) and B(-/+) electrodes that always have opposite phase of AC voltage, the emitted blue light appeared from the electrode areas covered by the bridging water (Movie S1, Supporting Information).

These results can be understood in terms of an initial coplanar (A–g–B) capacitor turning into two parallel plate capacitors with the phosphor (Ph) layer sandwiched within both of the newly formed capacitors. Each of these sandwiched capacitors formed with the polar electrode bridge (PEB) is connected in series, e.g., A–Ph–PEB and PEB–Ph–B, where the bridging liquid plays both the role of effective electrode above the Ph layer, and at the same time the role of a bridging connector. Hence, wetting converts the coplanar “A–g–B” dry capacitor into a circuit of two out-of-phase capacitors.

The dipoles of the PEB electrodes on top of the A and B capacitor electrodes are oppositely polarized during AC excitation, and the direction of the dipoles rotates across the width of the gap, as illustrated in Figure S1 (Supporting Information). As a result of the polarized liquid and the electrode bridge, the electric field in the phosphor layer is dramatically increased, by approximately one half of the ratio of the gap length to the combined thickness of the phosphor and dielectric layers.

During each half cycle of the PEB-ELS, electrons in the first capacitor A(+)-Ph-PEB(-) are accelerated downward across the phosphor layer from the PEB(-) side to the A(+) electrode, causing luminescence by impact excitation of Cu²⁺ luminophores. Simultaneously, electrons in the second capacitor PEB(+)-Ph-B(-) are accelerated in the opposite direction, upward from the B(-) electrode toward the PEB(+), causing impact excitation, luminescence, and filling traps at the interface between Ph and PEB (Figure S1, Supporting Information). Bridging is extremely important for equilibrating the electric potentials of the PEB electrodes, PEB(-) and PEB(+) over the A and B metallic electrodes. When the droplets of water, playing the roles of PEB(-) and PEB(+), are separated and not bridged, each of them will accumulate a “space charge” (e.g., by electrons leaking from the interfacial traps into the liquid) preventing accelerated movement of electrons due to the limited electrical field inside a A(+)-Ph-PEB “space charged” capacitor. Using water as the bridging electrode, the device luminance of PEB-ELSs (60.4 cd m⁻² at 120 V) is similar to that of the conventional sandwich electroluminescence device (64.5 cd m⁻² at 60 V). The applied voltage for the PEB-ELS is twice that of a conventional sandwich device since the PEB-ELS is functioning as two EL devices that are in series.

We evaluated polar and nonpolar liquids having a wide range of dielectric constants (*K*) and conductivities as the bridging electrode for PEB-ELS panels. Pouring drops of low dielectric constant liquids (toluene, *n*-hexane, 1,4-dioxane, or diethyl ether) on the PEB-ELS panel of Figure 1c,d produced no

noticeable light emission for the applied 2 kHz, 80 V electrical input to the panel (Figure 2b, bottom). However, under the same conditions, pouring 0.05 wt% aqueous NaCl, DI water, ethanol, or ethylene glycol (whose lowest DC dielectric constant is 24.55 for ethanol) caused the display to emit light in electrode regions of the panel where these liquids bridged between electrodes (Figure 2b, top).

Figure 2c compares the dependence of luminescence on voltage for various organic and aqueous polar electrode bridge liquids when a 2 kHz voltage is applied to the panel of Figure 1a, which has 1.5-mm-wide electrodes and 0.4 mm electrode gaps. The effects of electrode width and gap width on performance are shown in Figure S6 (Supporting Information). These results for DI water, aqueous NaCl solutions, ethanol (EtOH), and ethylene glycol (EG) show that similar luminescence results for polar liquids having a wide range of ionic conductivities (from $\approx 1.4 \times 10^{-5} \mu\text{s cm}^{-1}$ for ethanol to $\approx 4.75 \times 10^3 \mu\text{s cm}^{-1}$ for 0.25 wt% aqueous NaCl solutions). For example, at 120 V, the luminance of the devices contacting NaCl solution (0.05 wt%), DI water, EtOH, and EG was 62.4, 60.4, 52.3, and 49.6 cd m⁻², respectively. As shown in Figure 2c, the luminance increases with increasing concentration of NaCl in aqueous solutions. However, 0.05 wt% aqueous NaCl gave higher luminance than did the following four liquids when tested at 2 kHz (NaCl solution (0.05 wt%), DI water, EtOH, and EG). The luminescence obtained from the DI-water-based and EtOH-based PEB-ELSs rose to 103.6 and 92.1 cd m⁻², respectively, at a higher voltage (180 V at 2 kHz).

To further examine the modulating effects of liquids having various ionic conductivities, we measured the voltage dependence of luminescence when using as bridging electrode aqueous solutions containing NaCl concentrations of 0, 0.05, 0.10, and 0.25 wt%. The luminescence from all of the devices was very similar under the same applied voltages (60–178 V) at 2 kHz (Figure 2c), despite large differences in solution conductivity (conductivity of pure DI water: $<10 \mu\text{s cm}^{-1}$; 0.05 wt% NaCl: $\approx 1000 \mu\text{s cm}^{-1}$; 0.10 wt% NaCl: $\approx 2000 \mu\text{s cm}^{-1}$; 0.25 wt% NaCl: $4750 \mu\text{s cm}^{-1}$). Thus, the intrinsic ionic conductivity of the modulating material was not the determining factor affecting device performance. Notably, however, high current overloads resulting from the most highly conductive aqueous NaCl solutions (0.10 and 0.25 wt%) eventually led to irreversible damage of the electroluminescent layer.

The results of Figure 2d show that the luminance at 2 kHz and 160 V monotonically decreases with increasing impedance of the PEB-ELS for device impedances above 24 k Ω , where the measurements are for a 15×21 cm area of the device panel of Figure 2a. The device impedance at frequency ω is $Z = (Z'^2 + Z''^2)^{1/2}$, where Z' is the resistive component and $Z'' = 1/\omega C$ is the imaginary component due to device capacitance C . One might think that the current through the electroluminescent layer of the PEB-ELS is just inversely proportional to this device impedance. However, this is not the case. Even in the absence of the bridging dipolar layer, the impedance of the device at 2 kHz was 40.7 k Ω . Figure 2e shows the dependence of luminance and power efficiency on applied voltage for different frequencies for a PEB-ELS panel using DI water as the polar electrode bridge. While the luminance increases with increasing voltage and increasing frequency, the power

efficiency reaches a peak with increasing voltage and then decreases, and the energy efficiency decreases with increasing frequency. These voltage and frequency dependencies have been previously observed and explained for conventional sandwich electroluminescent light sources.^[20–24] For example, when the cycle time becomes smaller than the lifetime of the excited luminophore (which is about 1 ms), efficiency decreases. The maximum luminance shown in Figure 2e was 138.4 cd m⁻², which was realized at 158 V and 4 kHz and the calculated power efficiency reached a maximum of 0.85 lm W⁻¹ at 100 V and 500 Hz.

While the deposition of continuous dielectric and electroluminescent layers between the separated, coplanar metallic electrodes at device bottom is convenient for fabrication, this similar magnitude of device impedance with and without a polar bridging electrode means that current is wastefully bypassing the electroluminescent layer without contributing to light emission. If separate electrode stacks were electronically isolated except for the polar electrode bridge, light emission efficiency could be substantially increased. Without such isolation, which adds cost to the fabrication process, the dependence of luminance on the impedance of the polar bridge (or, in more detail, the real and imaginary contributions to this impedance with respect to the real and imaginary intrastack and interstack impedance contributions) becomes too complicated to be presently analyzed.

The functionally useful bridging material for an operational two-stack or multiple-stack coplanar electrode ELS is not limited to polar liquids. We evaluated graphite, a thin layer of

evaporated aluminum or gold, and a deposited zinc powder as bridging electrodes, all of which were directly applied on top of the devices (such as the large area device array shown in Figure 1c–e). Even when largely nontransparent, as long as the bridging material enabled sufficient interstack current flow between the two coplanar electrodes, the corresponding PEB-ELSs emitted some light, especially from the points at which the powder or film was in good contact with the phosphor layer.

Most interestingly, using an ordinary graphite pencil (like used to deposit graphene sheets)^[25] to draw on the panel of Figure 1c,d, a light-emitting redrawing of Picasso's images of birds was produced using a Martel C7401 pencil (Figure 2f). Broad shaded areas made using this pencil were lighter in visual appearance with voltage off, and brighter in light emission with voltage on than for shaded areas made using charcoal-based Martel pencils, which likely results from the relatively high electrical conductivity and transparency of stacked graphene layers compared to that for charcoal.

The pictures in Figure 3 show that a DI-water-saturated polyacrylamide hydrogel (which is a soft, flexible, optically transparent polymer) functions very effectively as a polar electrode bridge for a PEB-ELS. For this experiment, we fabricated two half devices by effectively, cutting a PEB-ELS in half (Figure 3a), leaving only a single electrode in each configuration. Two 4-mm-wide, 78-mm-long half-ELS cells (Figure 3b,c) were immersed in two beakers containing DI water and then separately connected to a 120 V, 2 kHz power source. No light emission occurred for any applied voltage or frequency (Figure 3c) until a hydrogel bridge was used to connect the water in the

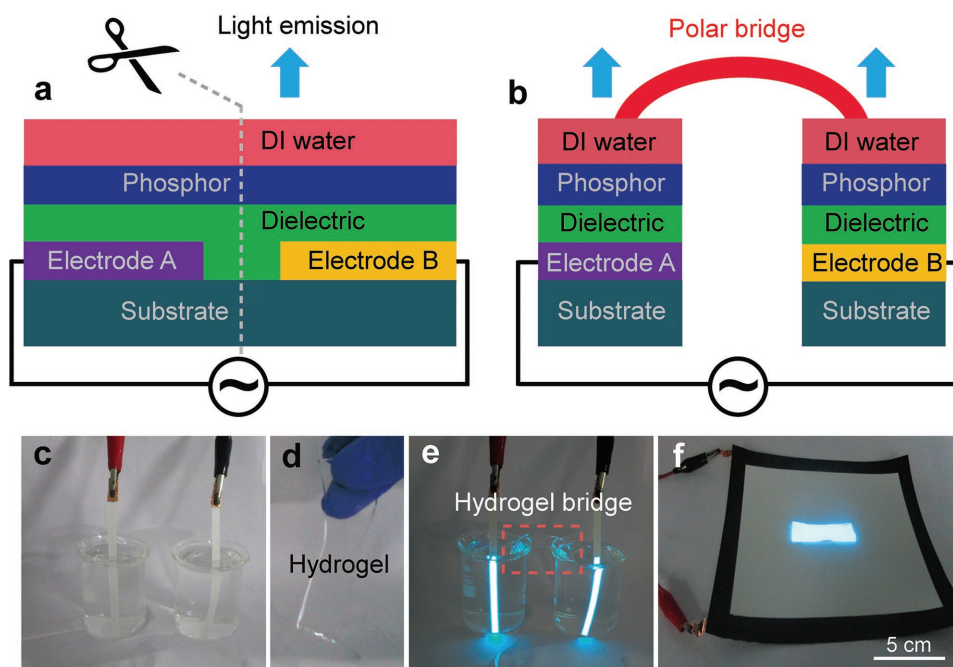


Figure 3. Polar electrode bridge experiments using half-PEB-ELSs. a) Schematic representation of a PEB-ELS incorporating a single polar electrode bridge of DI water. b) Schematic representation of a polar electrode bridge, made of a hydrogel, connecting two half-PEB-ELSs that are in two separate baths of DI water. c–e) Photographs of c) two half-devices in separate beakers, which do not emit any light when each half-device is attached to a 120 V, 2 kHz power source. d) An optically transparent, DI-water-saturated hydrogel and e) two half-devices emitting light in separate beakers when the water in the beakers is connected by using the hydrogel as a polar bridge. f) Photograph of the panel of Figure 1c,d, emitting light from the region contacted by a DI-water-saturated polyacrylamide hydrogel.

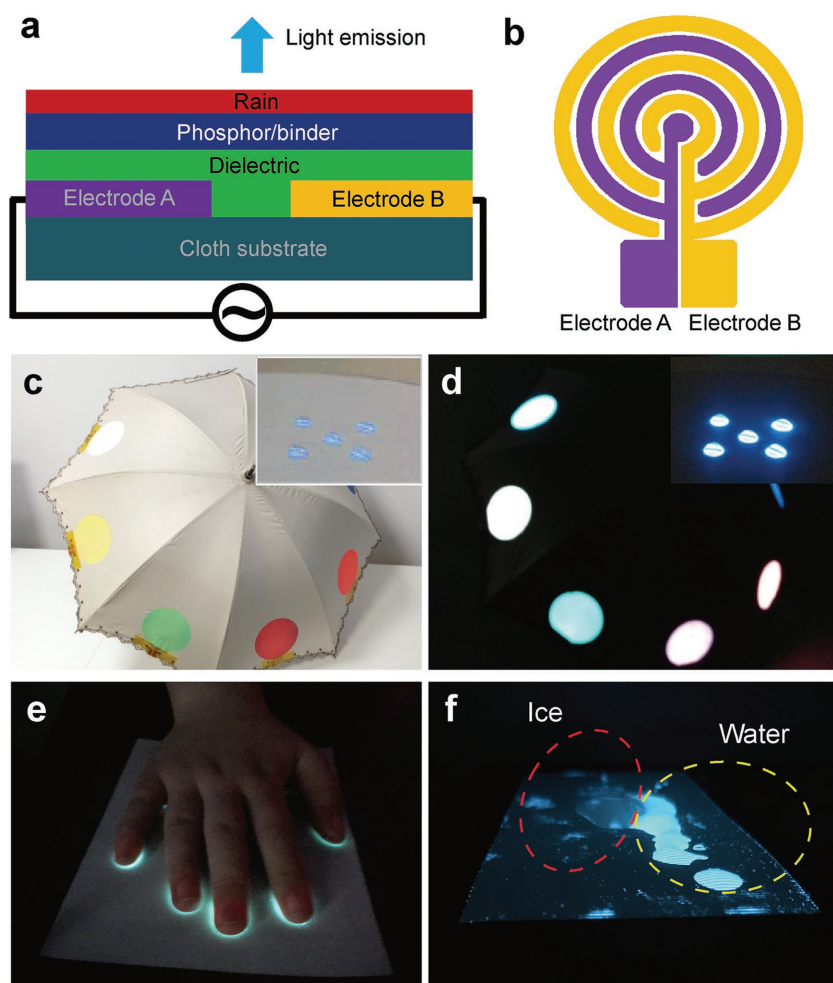


Figure 4. Schematic representations of a,b) the structure of a PEB-ELS-based rain sensor that uses semicircular interdigitated electrodes. c) Photograph of an umbrella containing seven circular rain sensors. The inset is a magnified view of light emission from five water droplets on the area of one sensor. d) Photograph in the dark of the umbrella of (c) when fully wet. The inset is a magnified view of light emission from five water droplets on the area of one sensor when viewed in the dark. e) Light emission resulting from the use of a human hand as a polar electrode bridge for the panel of Figure 1c,d. f) Photograph showing the decreased luminance from water electrode bridges when the water freezes.

two beakers, via a 5.0-cm-long, 1.6-cm-wide, and 0.3-mm-thick hydrogel strip (Figure 3e and Movie S2, Supporting Information). Moreover, the light emission from these light sources depended only weakly on the length of the hydrogel bridge that connected the two beakers, as this length was increased to 20 cm. Overlaying this DI-water-containing hydrogel onto an 8.0 cm² area of the panel type shown in Figure 1c,d (Figure 3f) provided a luminescence of 51.2 cd m⁻² at 120 V and 2 kHz, which is comparable to that obtained using a coating of DI water (62.4 cd m⁻² in Figure 2c).

Figure 4a–c illustrates and pictures the application of PEB-ELs as light-emitting panels on an umbrella, which automatically emit light when it rains. This application is conveniently made possible because the PEB-ELs are made of commercially available printable inks that are commonly used in printed electronics, which can be printed on diverse substrates—even on the nylon taffeta of an umbrella. In addition, the color of emitted

light can be changed by either changing the phosphor or using color conversion materials, like dyes or fluorophores (Figures S4 and S5, Supporting Information). At present, most commercial rain sensors are based on a mechanical response, a change in resistance, or disturbance in the reflective light passing into optical sensors. The present rain sensor directly causes light emission, since the rain acts as a polar electrode bridge. Each of the seven circular PEB-ELS rain sensors was directly screen printed onto the acrylic-coated nylon taffeta of the umbrella by sequentially adding the following layers: 1) circular-shaped interdigitated silver electrodes (diameter: 100 mm; width: 0.5 mm; interelectrode gap: 0.4 mm), as illustrated in Figure 4b; 2) a nonsegmented circular BaTiO₃/binder layer; and 3) a nonsegmented ZnS:Cu/binder layer that incorporates the phosphor needed to produce the desired color of light emission. Figure 4c,d shows the fabricated rain sensing umbrella in daylight and in the dark, where the insets show light emission from five rain drops that are on one of the umbrella sensors. Only light emission from wet sensor patches are visible in the main photograph of Figure 4d. Interestingly, touching fingers directly on the surface of the panel of Figure 1c,d also results in light emission (Figure 4e).

Another application of PEB-ELS devices might be remote optical detection of materials accumulated on a surface. For the purpose of this discussion, we call a device a PEB-ELS as long as it has the potential to emit light when contacted on its top surface by a polar liquid (or even an electronic conductor having sufficient lateral extent). As one example, Figure 4f shows that the freezing of water on the surface of a PEB-ELS causes a change in emitted light intensity, so

both the existence of water and whether or not it is partially or completely frozen could be remotely optically detected. Figure S3 (Supporting Information) shows that the light emission of an oil and water mixture on the surface of a PEB-ELS enables remote optical detection of the pattern of oil and water overcoating, since only the water-coated areas emit light. Especially, since the emission spectra of a PEB-ELS depend somewhat on the applied voltage and frequency and different areas of the electroluminescent layer can use different phosphors or fluorophores, it should be possible to remotely obtain greater information about accumulated materials on the 2D surface of a PEB-ELS by remotely detecting spectral regions in which emitted wavelengths are being partially absorbed.

In conclusion, we have developed a new type of flexible electroluminescent device that does not require transparent electrodes, and can be inexpensively fabricated by screen printing. After characterizing and explaining the effect of the

polar electrode bridge on performance, we have demonstrated application of these PEB-ELs as optically monitored sensors, which detect the presence of a polar material on the surface of the PEB-ELs and respond by emitting light at desired frequencies. Demonstrations include large PEB-EL arrays on an umbrella that lights up when it rains, a PEB-EL that lights up the contact zone when touched by a bare hand, a PEB-EL that indicates if a polar bridge liquid has frozen, and a PEB-EL that indicates the spatial distribution of polar and nonpolar liquids on the PEB-EL surface. This novel dual-stack, coplanar-electrode device geometry is extended to make displays causing light emission from a figure drawn using a graphite pencil, as well as organic light-emitting diodes and polymer light-emitting diodes that do not require transparent input and output electrodes.

Experimental Section

Fabrication of a PEB-ELs: Commercial polyester screens were used for the screen-printing apparatus. The screens were 40 × 70 cm and had a screen count of 300 mesh (i.e., 300 filaments per square inch, corresponding to ≈58 μm openings between mesh filaments). Two types of screens patterns were prepared. Pattern A for the interdigitated electrode was 17 × 22.5 cm and used various gap widths and electrode widths. Pattern B, for dielectric and phosphor printing, was 16 × 21 cm and had no filled squares. Flexible PET films were used as substrates, unless mentioned otherwise. To a PET film base, silver paste (70 wt% silver flakes suspended in binder from Henkel Asia) was screen printed as the interdigitated electrode using pattern A. A dielectric layer of BaTiO₃ (0.6–1.0-μm-thick from a 1:1 by weight dispersion in binder purchased from Shanghai Aladdin Biochem Technology), a phosphor layer of ZnS:Cu (10–30-μm-thick from a 1:1 weight dispersion from Lonco Company), and a cyanoresin binder layer (Nanjing Collaborative Innovation Lighting) were printed on top of the interdigitated electrode sequentially using the screen with pattern B. After each screen printing process, the corresponding printed layers were dried and annealed at 100 °C for 15 min. The average thicknesses of the Ag, dielectric, and phosphor layers were ≈8–10, 20, and 30 μm, respectively (Figure S2, Supporting Information).

DI-Water-Saturated Hydrogel: The acrylamide hydrogel was prepared by first mixing an aqueous solution of acrylamide (14 wt% in deionized water) with a crosslink agent (*N,N'*-methylenebisacrylamide, 0.0085 wt%) under vigorous stirring for 10 min. The thermo-initiator (ammonium persulfate, 0.14 wt%) and the accelerator (*N,N,N',N'*-tetramethylethylenediamine, 0.035 wt%) were then added into the mixture under vigorous stirring for 20 min. The mixture solidified into a gel when held at room temperature for 6 h. The 1.5–3.0-mm-thick gel was then cut into desired shapes.

Supporting Information

Supporting Information is available from the Wiley Online Library or from the author.

Acknowledgements

The authors thank L. Guo, X. Kuang, H. Yu, and J. Cao for assistance with the experimental set-up and sample preparation; X. Zhang, S. Chen, D. Luo, Y. Li, F. He, Y. Guo, and J. Miao for assistance with measurements and data analyses; and Prof. Z. Bao for important discussions. Financial support was from the Guangdong Talents Project, the National Basic Research Program of China (973 Program, No. 2015CB856505),

the Shenzhen Peacock Program (KQTD2014062714543296), the Guangdong Provincial Science Technology Project (2015B090914002), the China (Shenzhen)-Israel Technology Collaboration Project (GJHZ20170313145720459), and the Shenzhen Science and Technology research grant (JCYJ20160510144254604).

Conflict of Interest

The authors declare no conflict of interest.

Keywords

AC displays, electroluminescence, polar electrodes, sensors

Received: June 26, 2017

Revised: August 9, 2017

Published online: September 12, 2017

- [1] L. Hu, M. Pasta, F. La Mantia, L. Cui, S. Jeong, H. D. Deshazer, J. W. Choi, S. M. Han, Y. Cui, *Nano Lett.* **2010**, *10*, 708.
- [2] J. Kim, D. Son, M. Lee, C. Song, J.-K. Song, J. H. Koo, D. J. Lee, H. J. Shim, J. H. Kim, M. Lee, T. Hyeon, D.-H. Kim, *Sci. Adv.* **2016**, *2*, e1501101.
- [3] J. Reeder, M. Kaltenbrunner, T. Ware, D. Arreaga-Salas, A. Avendano-Bolivar, T. Yokota, Y. Inoue, M. Sekino, W. Voit, T. Sekitani, T. Someya, *Adv. Mater.* **2014**, *26*, 4967.
- [4] S. Il Park, D. S. Brenner, G. Shin, C. D. Morgan, B. A. Copits, H. U. Chung, M. Y. Pullen, K. N. Noh, S. Davidson, S. J. Oh, J. Yoon, K.-I. Jang, V. K. Samineni, M. Norman, J. G. Grajales-Reyes, S. K. Vogt, S. S. Sundaram, K. M. Wilson, J. S. Ha, R. Xu, T. Pan, T.-I. Kim, Y. Huang, M. C. Montana, J. P. Golden, M. R. Bruchas, R. W. Gereau 4th, J. A. Rogers, *Nat. Biotechnol.* **2015**, *33*, 1280.
- [5] B. C. K. Tee, A. Chortos, A. Berndt, A. K. Nguyen, A. Tom, A. McGuire, Z. C. Lin, K. Tien, W.-G. Bae, H. Wang, P. Mei, H.-H. Chou, B. Cui, K. Deisseroth, T. N. Ng, Z. Bao, *Science* **2015**, *350*, 313.
- [6] C. Wang, D. Hwang, Z. Yu, K. Takei, J. Park, T. Chen, B. Ma, A. Javey, *Nat. Mater.* **2013**, *12*, 899.
- [7] S. Bauer, S. Bauer-Gogonea, I. Graz, M. Kaltenbrunner, C. Keplinger, R. Schwödiauer, *Adv. Mater.* **2014**, *26*, 149.
- [8] F. Ilievski, A. D. Mazzeo, R. F. Shepherd, X. Chen, G. M. Whitesides, *Angew. Chem. Int. Ed.* **2011**, *123*, 1930.
- [9] J. Y. Kim, K. Lee, N. E. Coates, D. Moses, T.-Q. Nguyen, M. Dante, A. J. Heeger, *Science* **2007**, *317*, 222.
- [10] C. S. Haines, M. D. Lima, N. Li, G. M. Spinks, J. Foroughi, J. D. W. Madden, S. H. Kim, S. Fang, M. J. de Andrade, F. Göktepe, O. Göktepe, S. M. Mirvakili, S. Naficy, X. Lepró, J. Oh, M. E. Kozlov, S. J. Kim, X. Xu, B. J. Swedlove, G. G. Wallace, R. H. Baughman, *Science* **2014**, *343*, 868.
- [11] J. A. Lee, A. E. Aliev, J. S. Bykova, M. J. de Andrade, D. Kim, H. J. Sim, X. Lepró, A. A. Zakhidov, J.-B. Lee, G. M. Spinks, S. Roth, S. J. Kim, R. H. Baughman, *Adv. Mater.* **2016**, *28*, 5038.
- [12] Y. Z. Wang, D. D. Gebler, L. B. Lin, J. W. Blatchford, S. W. Jessen, H. L. Wang, A. J. Epstein, *Appl. Phys. Lett.* **1996**, *68*, 894.
- [13] L. J. Meng, C. H. Li, G. Z. Zhong, *J. Lumin.* **1987**, *39*, 11.
- [14] Y. S. Chen, D. C. Krupka, *J. Appl. Phys.* **1972**, *43*, 4089.
- [15] J. F. Wager, P. D. Keir, *Annu. Rev. Mater. Sci.* **1997**, *27*, 223.
- [16] C. Larson, B. Peele, S. Li, S. Robinson, M. Totaro, L. Beccai, B. Mazzolai, R. Shepherd, *Science* **2016**, *351*, 1071.
- [17] H. Li, Q. Zhao, W. Wang, H. Dong, D. Xu, G. Zou, H. Duan, D. Yu, *Nano Lett.* **2013**, *13*, 1271.

- [18] Q. Pei, G. Yu, C. Zhang, A. J. Heeger, *Science* **1995**, 269, 1086.
- [19] A. N. Aleshin, I. P. Shcherbakov, V. N. Petrov, *Solid State Commun.* **2015**, 208, 41.
- [20] O. A. Yoshimasa, *Electroluminescent Displays*, World Scientific, MA, USA **1995**.
- [21] A. Kitai, *Luminescent Materials and Applications*, Hoboken, NJ, USA **2008**.
- [22] P. D. Rack, P. H. Holloway, *Mater. Sci. Eng., R* **1998**, 21, 171.
- [23] R. Mach, G. O. Muller, *Phys. Status Solidi* **1984**, 81, 609.
- [24] A. G. Fischer, *J. Electrochem. Soc.* **1963**, 110, 733.
- [25] I. Janowska, F. Vigneron, D. Bégin, O. Ersen, P. Bernhardt, T. Romero, M. J. Ledoux, C. Pham-Huu, *Carbon* **2012**, 50, 3106.